

# TSUNAMI WAVEFORM INVERSION OF THE 2010 CHILEAN EARTHQUAKE

César Jiménez

Assistant Professor, Universidad Nacional Mayor de San Marcos, Perú  
cjimenezt@unmsm.edu.pe

**Abstract:** The 2010 Chile earthquake occurred off the coast of the Maule Region in the south-central Chile on February 27th, 2010, at 03:34 local time (06:34 UTC) with a magnitude of Mw8.8. As a coseismic effect, tsunami waves were triggered and destroyed several coastal towns and ports. In this paper, from the analysis and digital processing of 10 tide gauge records we obtained the initial coseismic deformation parameters through a tsunami waveform inversion process. The maximum slip obtained is 19.5m near to the latitude 35.5S, in the northern part of the rupture area. The scalar seismic moment calculated is  $2.02 \times 10^{22}$  Nm; an equivalent to the Mw8.8. As a result, we propose a new heterogeneous model of the seismic source as an initial condition for future tsunami simulations related to this event.

**Keywords:** tsunami, earthquake, inversion.

## 1. INTRODUCTION

The 2010 Chile earthquake occurred off the coast of the Maule Region, in the limits of the Nazca plate and the South American plate. These tectonic plates converge at a rate of 8 cm per year (DeMets, 1990), with the Nazca plate in a subduction process under the South American plate. An inverse fault mechanism has triggered many earthquakes around this area, with an average of at least one major earthquake of magnitude over Mw8.0 in the last five centuries (Madariaga, 1998).

In this paper, we propose a seismic source or coseismic deformation model, and we present the simulation of the related tsunami and its parameters such as: arrival time, wave amplitude, first wave polarity and in general the waveform in a good correlation with the tide gauge records for the available stations.

## 2. DATA

### 2.1 Tide gauge and DART buoy records

We obtained 09 tide gauge station records from the Sea Level Station Monitoring Facility (IOC, 2011), located in general near ports or creeks in the coast. Also a DART buoy of the National Data Buoy Center (NOAA, 2011) located offshore. All of these stations are within Peru and Chile coastal areas. See Fig.1.

### 2.2 Digital Processing of Tidal Signals

Tide gauge signals hold a wide range of frequency spectrum with three principal components: tide, surge and tsunami waves. Consequently, it is necessary to apply several digital processing algorithms to these signals (Jimenez, 2007). First, a data interpolation is conducted to resample the signal into 1min interval using the splines interpolation method.

Then, the average value is subtracted to center the signal with respect to the horizontal axis. Next, a Butterworth high-pass filter is applied to eliminate long periods of tides and a low-pass filter to eliminate short periods of surge. Finally, the time is adjusted to the origin time of the earthquake (Rabinovich et al., 2006). However, for the inversion method, all the records are synchronized to an arrival time equally to the minimum arrival time of the available stations. See Table1.

Table 1. Tide gauge and DART buoy stations are in order from south to north. Arrival Time  $T_a$  is in reference to origin time of the earthquake.

N°	Station	Lat °	Lon °	Ta(min)
1	Ancud	-41.867	-73.832	88
2	Talcahuano	-36.695	-73.106	20
3	Valparaíso	-33.027	-71.626	20
4	Coquimbo	-29.950	-71.335	55
5	Caldera	-27.065	-70.825	76
6	Antofagasta	-23.653	-70.404	106
7	Iquique	-20.205	-70.148	140
8	Arica	-18.476	-70.323	163
9	Dart 32412	-17.975	-86.392	189
10	Callao	-12.071	-77.174	243

### 2.3 Bathymetry data

For the bathymetry data, GEBCO (GEBCO, 2011) data was used with a 30 arc second accuracy or 927m shown in Fig.1. In the case of Callao station, 3 arc second or 92m data obtained through bathymetry survey and provided by the Dirección de Hidrografía y Navegación (DHN)-Peru.

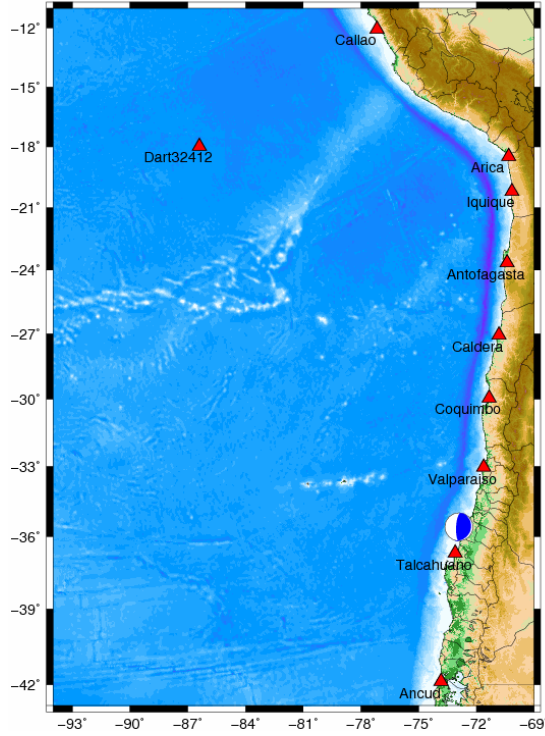


Fig. 1. Bathymetry, tide gauge and DART buoy stations.

### 3. INVERSION METHOD

In this paper, tide gauge and DART buoy records of tsunami are used to estimate the slip distribution (parameter of source). The process is considered as a “Linear time-invariant system”, with two important properties: a) Linearity. It allows the use of superposition of the Green functions and unitary deformations. b) Time related invariance. It allows a displacement of time for record signals and its correspondent Green functions, to synchronize arrival times to the minimum arrival time of tide gauge and DART buoy records. This also allows the use of tide gauges independently to its distance to the event epicenter. There is not a unique solution for the inverse problem, however the group of values with better correlation with the observe data is selected.

#### 3.1 Source parameters

To estimate the slip distribution we used the inversion method for 10 records of tide gauge and DART buoy with acceptable quality (Satake and Kanamori, 1991). The rupture area was divided in 10 pieces of equal dimension ( $L=90\text{km}$ ,  $W=50\text{km}$ ), each of them located at an  $H_j$  depth related to the upper part of each sub-fault. The coseismic deformation is calculated for each sub-fault with unitary slip, following formulations by Okada (Okada 1985) and data from the focal mechanism. Parameters

of focal mechanism are taken from the Global CMT (see Table III) and are the same for each sub-fault.

Table 3. Focal mechanism parameters.

Strike angle	$18^\circ$
Dip angle	$18^\circ$
Slip angle	$104^\circ$

#### 3.2 Green functions

A Green function represents the system response (the  $i$ -th station) to a unitary disturbance (unitary slip of the  $j$ -th sub-fault). Through these group of deformations as initial condition, the waveforms (Green functions) are calculated at each station in the tsunami simulation per sub-fault.

The observed waveforms are expressed as a linear combination of the calculated waveforms using tensorial notation:

$$G_{ij}(t) * m_j = d_i(t) \quad (1)$$

where,  $G_{ij}$  is the Green function of the  $i$ -th station generated by the  $j$ -th sub-fault,  $m_j$  is the slip value in the  $j$ -th sub-fault,  $d_i$  is the observed signal at the  $i$ -th station.

TUNAMI model (Imamura 1995) was used as the tsunami propagation model with one grid to obtain Green functions to stations in Chile and the DART buoy. In the case of Callao (Peru) station, four nested grids were used to take advantage of the available fine bathymetry data. The limits of the most coarse grid are:  $-10.0$  (top latitude),  $-41.0$  (bottom latitude),  $-92.0$  (left longitude),  $-69.0$  (right longitude).

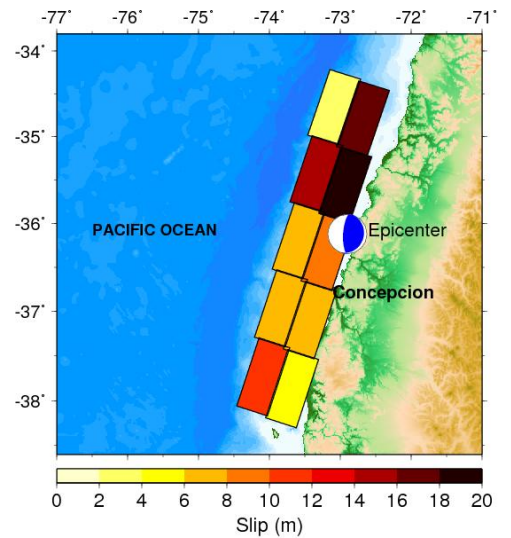


Fig. 2. Sub-fault distribution and slip amounts. The maximum slip (19.5m) is located in the northern part of the rupture area.

### 3.3 Inversion

The inversion process is conducted using the non-negative least square method (Lawson et al, 1974). This method compares the simulated signal and the observed one until the square of the difference is minimum under the condition of  $m_j > 0$ .

$$|G_j m_j - d_i|^2 \rightarrow 0 \quad (2)$$

Only the first part of the signal should be taken into account to avoid noises in the signal, such as effects of wave reflection or local resonances due to bathymetry and coastline morphology near stations. In this case an interval of time from 20min to 90min was considered to perform the inversion calculation.

The algorithm should consider the physical definition of a positive slip value, even though the positive result may not be the optimum value from the least square method point of view.

## 4. RESULTS AND DISCUSSION

Results of the inversion are shown in Table 4 and Figure 3. From the slip values the total deformation field is obtained as a linear combination of the unit deformations. This is the initial condition for tsunami propagation simulations. The maximum value for the slip is 19.5m in the northern part of the rupture area (sub-fault No.08). This result is in agreement with observed damages after the earthquake, the city of Concepcion (north to the fault - Lat. 35.32S) was one of the most affected area by the tsunami. This city is in the middle of sub-faults No.08 and No.10. Also the maximum value for the initial coseismic deformation is calculated to 6.39m.

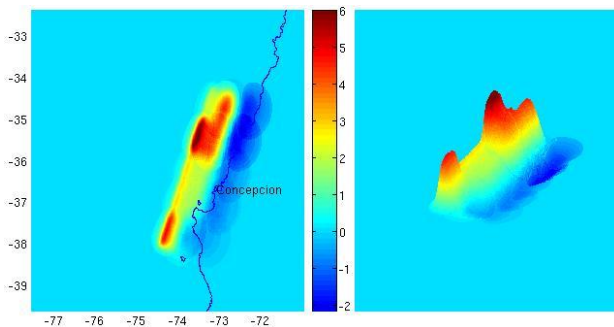


Fig. 3. Vertical displacement (en meters) of sea floor and land surface as used in tsunami source model. Left (2D). Right (3D).

Table 4. Slip distribution for each sub-fault. Coordinates are from the lower left corner and depth to the upper part of the sub-fault. ( $M_0$  is in  $10^{21}$  Nm).

N°	Lat	Lon	H <sub>i</sub> (km)	Slip(m)
1	-38.060	-74.460	12.00	11.63
2	-38.192	-74.053	27.45	04.25
3	-37.290	-74.210	12.00	06.35
4	-37.422	-73.803	27.45	07.86
5	-36.520	-73.960	12.00	06.32
6	-36.653	-73.553	27.45	08.85
7	-35.751	-73.710	12.00	14.04
8	-35.883	-73.303	27.45	19.47
9	-34.981	-73.459	12.00	03.81
10	-35.113	-73.053	27.45	17.16

Due to the location of the epicenter and the geometry of the rupture area, it is easy to observe that the process of rupture had two directions: from the epicenter to the north with the major deformation and from the epicenter to the south. Deformation distribution, Figure 3, agrees with previous sources calculated by methods of teleseismic inversion (Lay et al, 2010) and geodesic-teleseismic (Sladen 2010), however these last two methods show lower slip values. And also, agrees with joint inversion (seismic, geodetic and tsunami) from Lorito (Lorito et al, 2011).

### 4.1. Scalar seismic moment

With the slip distribution and every sub-fault dimension, it is possible to calculate the scalar seismic moment through:

$$M_0 = \mu LWD \quad (3)$$

$$M_w = \frac{2}{3} \log(M_0) - 6.07 \quad (4)$$

where,  $M_0$  is the seismic moment in Nm,  $\mu$  is the shear modulus of value  $4.0 \times 10^{10}$  N/m<sup>2</sup>,  $L$  the length of sub-fault, fixed at 90km,  $W$  width of 50km and  $D$  the slip. Using results from Table 4, the seismic moment results in  $M_0 = 2.02 \times 10^{22}$  Nm.

According to equation 4, the moment magnitude calculated for this source is Mw8.8, same as the USGS-NEIC report. This means that even from tide gauge and DART buoy records we may obtain a similar value with seismic records.

#### 4.2. Waveforms of the inversion method

Figure 4 shows the result of the waveform inversion method applied and the comparison of simulated and observed records. All signals have been displaced on time with respect to the arrival time in order to synchronize all arrival times to the minimum arrival time of stations (20 minutes in this case). A good correlation is observed. This can be improved through the use of only DART buoys in the inversion method. DART buoys are located offshore where reflection and coastline resonance effects are not present. Unfortunately for this area of the world there are not enough buoys or they are too far from the seismic source.

In Table 5 the correlation coefficient between the observed and simulated signals of stations is shown. Arica, Iquique and Antofagasta stations resulted with better correlation values, while Talcahuano shows a low correlation. (Figure 4).

Table 5. Correlation coefficient between the observed and simulated signals.

N°	Station	Correlation
1	Ancud	0.71
2	Talcahuano	0.43
3	Valparaíso	0.77
4	Coquimbo	0.83
5	Caldera	0.68
6	Antofagasta	0.94
7	Iquique	0.96
8	Arica	0.96
9	Dart 32412	0.76
10	Callao	0.69

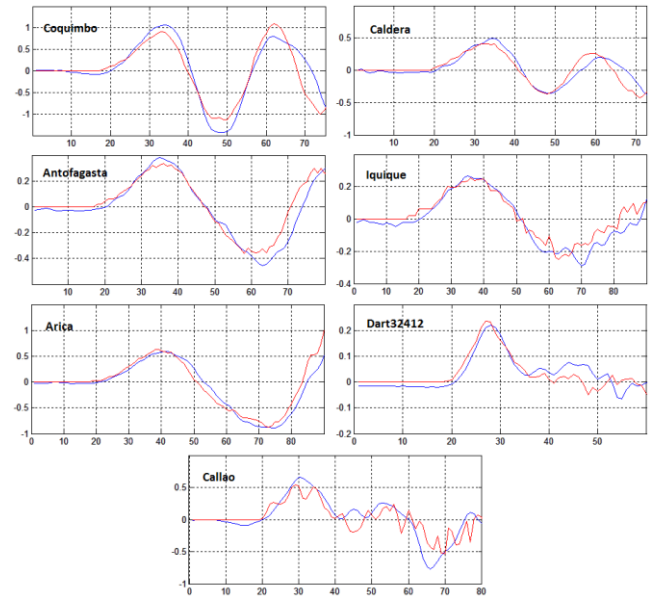


Fig. 4. Tide gauge and DART buoy records selected. Blue: observed; Red: simulated. Graphic of Height(m) vs Time(min).

## 5. CONCLUSIONS

A proposed heterogeneous source model of the 2010 Chilean earthquake was calculated using waveform inversion method from 10 stations available. Results showed a good agreement with slip distribution and seismic moment magnitude estimated by other methods.

The maximum initial coseismic deformation for this model is 6.39m and the maximum slip of 19.5m is located in the northern part of the rupture area. The scalar seismic moment was calculated to  $M_0 = 2.02 \times 10^{22}$  Nm and the magnitude inferred from tide gauge and DART buoy records was Mw8.8, similar to the results obtained by seismic records inversion.

The rupture mechanism for this earthquake was characterized as a bidirectional directivity from the epicenter, and a high energy concentration in the northern part compared to the southern part of the source.

The inverse problem has not an unique solution, therefore, values with better correlation between observed and simulated data were selected. In Arica, Iquique and Antofagasta stations results showed better correlations (0.96), while in Talcahuano a low correlation was found (0.43).

## REFERENCES

- CMT (2011). Global Centroid Moment Tensor Project: <http://www.globalcmt.org/>
- DeMets, C. and Gordon, R. and Argus, D. and Stein, S. (1995). Current plate motions. *Journal of Geophysical Research*, pages 425-478:101.
- GEBCO (2011). General Bathymetric Chart of the Oceans: <http://www.gebco.net/>
- Imamura, F. (1995). Review of tsunami simulation with a finite difference method. *Long Wave Runup Models*, World Scientific, pages 25-42.
- IOC (2011). Sea Level Station Monitoring Facility: <http://www.ioceaselevelmonitoring.org/>.
- Jimenez, C. (2007). Procesamiento digital de señales sísmicas con Matlab. (Spanish). *Revista de Investigacion de Fisica*, 10-2:23-28.
- Lawson, C. and Hanson, R. (1974). *Solving Least Squares Problems*. Prentice-Hall.
- Lay, T., Ammon, C., Kanamori, H., Koper, K., Sufri, O., and Hutko, A. (2010). Teleseismic inversion for rupture process of the 27 February 2010 Chile (Mw8.8) earthquake. *Geophysics Research Letters*, 37:L13301.
- Lorito, S. and Romano, F. and Atzori, S. and Tong, X. (1974). Limited overlap between the seismic gap and coseismic slip of the great 2010 Chile earthquake. *Nature Geosciences*, 1-5:NGEO1073.
- Madariaga, H. (1998). Sismicidad de Chile (Spanish). *Fisica de la Tierra*, 10:221-258.
- NOAA (2011). Data Buoy Center: <http://www.ndbc.noaa.gov/dart.shtml>
- Okada, Y. (1985). Surface deformation due to shear and tensile faults in a half space. *Bulletin of Seismological Society of America*, 75:1135-1154.
- Rabinovich, A., Thomson, R., and Stephenson, F. (2006). The Sumatra Tsunami of 26 December 2004 as observed in the North Pacific and North Atlantic Oceans. *Surveys in Geophysics*, 27-6:647-677.
- Satake, K. and Kanamori, H. (1991). Use of tsunami waveform for earthquake source study. *Natural Hazards*, 4:193-208.
- Sladen, A. (2010). A coseismic distributed slip model for the 2010 Mw 8.8 Maule (Chile) earthquake. *Proceedings of the Chapman Conference on Giant Earthquakes and their Tsunamis*. Chile.
- Suppasri, A., Imamura, F., and Koshimura, S. (2010). Effects of the rupture velocity of fault motion. *Coastal Engineering Journal*, 52-2:107-132.
- USGS-NEIC (2011). National Earthquake Information Center: <http://neic.usgs.gov>